Structural Engineering and Mechanics, *Vol. 56, No. 2 (2015) 169-188*
DOI: http://dx.doi.org/10.12989/sem.2015.56.2.169

Evaluating the spread plasticity model of IDARC for inelastic analysis of reinforced concrete frames

Mehdi Izadpanah[a] and AliReza Habibi[*]

Department of Civil Engineering, University of Kurdistan, Sanandaj, Iran

(Received April 5, 2015, Revised October 2, 2015, Accepted October 5, 2015)

Abstract. There are two types of nonlinear analysis methods for building frameworks depending on the method of modeling the plastification of members including lumped plasticity and distributed plasticity. The lumped plasticity method assumes that plasticity is concentrated at a zero-length plastic hinge section at the ends of the elements. The distributed plasticity method discretizes the structural members into many line segments, and further subdivides the cross-section of each segment into a number of finite elements. When a reinforced concrete member experiences inelastic deformations, cracks tend to spread form the joint interface resulting in a curvature distribution. The program IDARC includes a spread plasticity formulation to capture the variation of the section flexibility, and combine them to determine the element stiffness matrix. In this formulation, the flexibility distribution in the structural elements is assumed to be the linear. The main objective of this study is to evaluate the accuracy of linear flexibility distribution assumed in the spread inelasticity model. For this purpose, nonlinear analysis of two reinforced concrete frames is carried out and the linear flexibility models used in the elements are compared with the real ones. It is shown that the linear flexibility distribution is incorrect assumption in cases of significant gravity load effects and can be lead to incorrect nonlinear responses in some situations.

Keywords: lumped plasticity; distributed plasticity; reinforced concrete; flexibility distribution; gravity load effects

1. Introduction

The plasticity models are generally divided in two categories: lumped plasticity and spread plasticity. In the former, there are some proposed models such as "two component model", "one component model". The two component model is one of the first models proposed by Clough and Johnston (1966) and consists of a linear elastic member in parallel with an elastic perfectly plastic member. The most important lack of this model is that it cannot consider stiffness degradation. Aoyama and Sugano (1968) extended this model. In their proposed model, each element is divided into four parallel elements which consists of an elastic member and three elastoplastic members in parallel. The model is able to consider different cracking and yielding characteristics at the two critical end sections. Giberson (1967, 1969) suggested a one-component model. This model

∗Corresponding author, Associate Professor, E-mail: ar.habibi@uok.ac.ir
[a]Ph.D. Student, E-mail: m.eazadpanah@yahoo.com

http://www.techno-press.org/?journal=sem&subpage=8 ISSN: 1225-4568 (Print), 1598-6217 (Online)

consists of an elastic element with one nonlinear rotational spring at each end. The location of the springs is considered in places that yielding is expected. The inelastic deformation of each element is condensed into these rotational end springs. A major advantage of the model is that inelastic member-end deformation depends solely on the moment acting at the end so that any moment-rotation hysteretic model can be assigned to the spring. The weak spot of this model is ignoring the curvature distribution effects on the member-end rotation. The above mentioned model was amended by changing the location of the plastic hinges at the ends of the members to consider the effects of rigid end zones (Al-Haddad and Wight 1986).The performance of the one-component model is expected to be reasonably good for a relatively low-rise frame structure in which the inflection point of a column locates reasonably close to mid-height (Otani 1980). Giberson (1967) compared the one component model with the two-component model and showed that the one component model was more proper than the two-component model. Kunnath and Reinhorn (1989) proposed a concentrate plasticity model that was used in IDARC2D (Park *et al*. 1987) as an option for concentrated plasticity.

Although simplicity and computability are two advantages of the above listed lump plasticity models, due to their intrinsic zero-length plastic-zone assumption, they does not accurately represent the distribution of plasticity within individual members of the frame. To overcome this problem, discrete element models were proposed. In these models, the member can be subdivided into short line segments along the length, with each short segment assigned a nonlinear hysteretic characteristic. Each short segment is allocated a nonlinear hysteric stiffness characteristic. The nonlinear stiffness can be assigned within a segment, or at the connection of two adjacent segments. Wen and Janssen (1965) presented their models in this category. They introduced a multi-spring model for dynamic analysis of a plane frame. Powell (l975) put forward a degrading stiffness hysteresis model. In this model, shorter segments were recommended in a region of high moment, and longer segments in a low-moment region. These discrete element models are more accurate but they require more computational effort than other plasticity models. The latter model used for nonlinear behavior is the spread plasticity model. The spread plasticity models provide a more general framework for nonlinear structural analysis.

Against to the above mentioned discrete plasticity models, there are some continues models developed based on prescribed distribution pattern of flexural flexibility along the length of member. The parabolic-inflection distribution (Takizawa 1973) and linear-inflection distribution (Park *et al*. 1987) are in this category. In parabolic-inflection model, an elastic flexibility at the infection point is taken into account. This is an interesting concept for analyzing an inelastic member. However, the parabolic-inflection flexibility distribution may not describe the actual concentration of deformation at critical sections due to flexural yielding and deformation attributable to slippage of longitudinal reinforcement within a beam-column connection (Otani1980). The linear-inflection proposed by Park *et al*. (1987) was introduced in the original version of IDARC2D developed by Reinhorn *et al*. (2009). Although the parabolic-inflection and linear-inflection models can be efficient for some members, one of their defects is that they are dependent on location of inflection point. To solve this problem and improve the plasticity models, two spread plasticity models based on a linear flexibility distribution and a uniform flexibility distribution were proposed that in these two models, the flexibility varies only in inelastic zones while the rest of the member is elastic with constant flexibility (Kunnath and Reinhorn 1989).

Recently, Hajjar *et al*. (1998) put forward a distributed plasticity model for cyclic analysis of concrete-filled steel tube beam-columns and composite frames. They presented the constitutive formulation and cyclic analysis capability of a three-dimensional fiber-based distributed plasticity

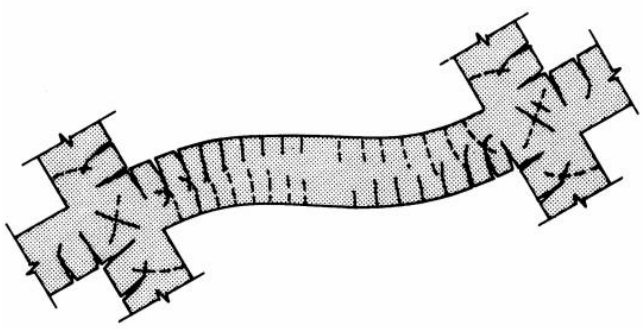

Fig. 1 Deformation of reinforced concrete beam under gravity and earthquake loads (Otani1980)

finite element for square or rectangular concrete-filled steel tube (CFT) beam-columns. They also used a distributed plasticity model for concrete filled steel tube beam-columns with inter layer slip (Hajjar *et al*. 1998). Kim and Kurama (2008) used the spread plasticity model to reflect flexural nonlinearity. The column and beam members were modeled using nonlinear beam-column elements. Alva and de Cresce El Debs (2010) applied a lumped dissipation model in nonlinear analysis of reinforced concrete structures. They considered the dissipation of energy of the reinforced concrete members as a consequence of concrete damage and steel reinforcement plasticity. As a simplification, it was supposed that the energy dissipation was restricted to plastic hinges at the ends of the member, while the rest of the member remains elastic. He and Zhong (2012) used the fiber section model to derive the nonlinear relation of section deformations and internal forces and their interaction. Birely *et al*. (2012) presented a model to simulate the nonlinear response of planar reinforced-concrete frames including all sources of flexibility. They modeled nonlinearity by introducing a dual-hinge lumped-plasticity beam element comprised two rotational springs in series; one spring simulates beam flexural response and one spring simulates joint response. Roh *et al*. (2012) proposed a power spread plasticity model for inelastic analysis of reinforced concrete structures and compared their plasticity model with linear plasticity model used in IDARC2D. Kucukleret *et al*. (2014) extended their stiffness reduction, to capture fully the detrimental influence of the spread of plasticity, residual stresses and geometrical imperfections on the capacity of columns and beam-columns. Nguyen and Kim (2014) presented a displacement-based finite element procedure for second-order spread-of-plasticity analysis of plane steel frames with nonlinear beam-to-column connections under dynamic and seismic loadings.

Since the assumed flexibility distribution pattern in the IDARC is violated when stress levels due to initial loads are relatively large, the main objective of this study is to evaluate the accuracy of this model for nonlinear analysis of reinforced concrete structures. To do so, the real flexibility of several structural elements with different load levels is determined and results are compared with the assumed plasticity model.

2. Reinforced concrete plasticity model

As it was mentioned, the proposed plasticity models are divided to two main categories: lump plasticity and spread plasticity. Now the main question is that which one is suitable for reinforced concrete members? Inelastic deformation of reinforced concrete structural elements does not

concentrate in a place and rather spread along the member as shown in Fig. 1. So it seems that the proposed lumped plasticity models cannot simulate the real distribution of stiffness within a reinforced concrete member.

Another choice in plasticity models is “discrete element method”. In this model, the member is subdivided into short line segment with assigned a nonlinear hysteretic characteristic for each short segment. The nonlinear stiffness can be assigned within a segment, or at the connection of two adjacent segments as shown in Fig. 2.

The accuracy of this model is enhanced when the number of segments rises; although the computational effort increases too. Choosing shorter segments should be based on moment distribution along the member and places with high moment but this selection is difficult when the moments are different at various load steps during nonlinear analysis. The other plasticity models are “spread plasticity models”. In this regard, one of the most popular models is the linear plasticity model used in IDARC2D (Reinhorn *et al*. 2009) (Fig. 3). This model has been used for inelastic analysis of reinforced concrete structures by many researchers. In fact, the main problem of these kinds of models (spread plasticity models) is that the flexibility distribution along the element is assumed to be merely based on lateral load apart from the gravity load effects. This assumption can lead to incorrect results in cases of significant gravity load moments.

Fig. 2 Discrete element model (a) multi-spring model (Birely *et al*. 2012) (b) multi-section model (Wen and Janssen1965)

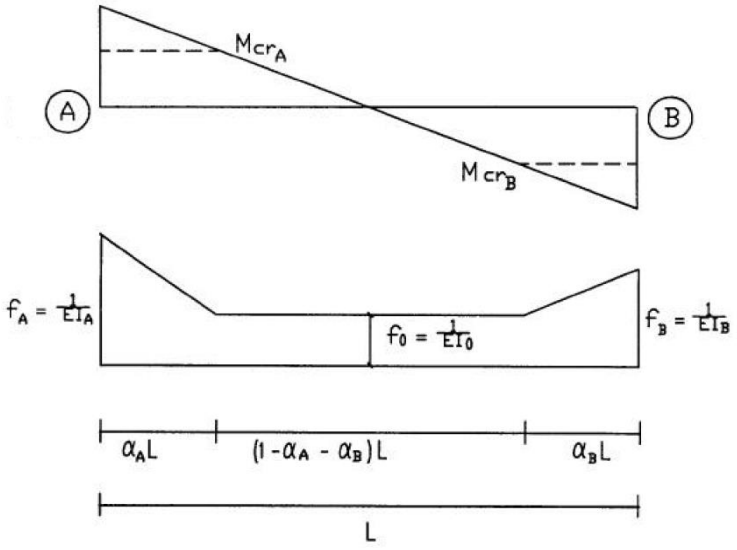

Fig. 3 Linear flexibility distribution model

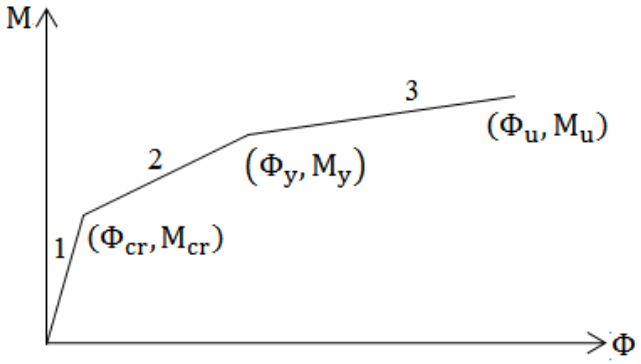

Fig. 4 Tri-linear moment curvature curve

3. Moment curvature curve

The moment-curvature relation of every RC structural element has a definitive effect on the behavior of the structure. The flexural stiffness of each member depends on moment curvature relation directly. So in this study, the tri-linear moment curvature relation, as shown in Fig. 4, is used to express the nonlinear behavior of reinforced concrete sections.

As it is evidence in the Fig. 4, the flexural stiffness can has three values based on the amount of bending moments. The moment curvature relation of a structural element highly depends on its cross-section. In this study, the column sections are limited to rectangle and that of beams can assume rectangle, *T* or *L* shaped. The moment-curvature relations used in the present study are similar to those utilized by Habibi and Moharrami (2010). The flexibility of each branch in the Fig. 4 can be specified as follows

$$\frac{1}{EI_0} = \left(\frac{M_{cr}}{\varphi_{cr}}\right)^{-1} \tag{1a}$$

$$\frac{1}{EI_{cr}} = \left(\frac{M_y - M_{cr}}{\varphi_y - \varphi_{cr}}\right)^{-1} \tag{1b}$$

$$\frac{1}{EI_y} = \left(\frac{M_u - M_y}{\varphi_u - \varphi_y}\right)^{-1} \tag{1c}$$

Where Eqs. (1a)-(1c) are used for zones of 1, 2 and 3 of M-φ curve, respectively. In Eq. (1) EI_0, EI_{cr} and EI_y are the flexural stiffness of different zones of moment curvature curve in Fig. 4 M_{cr}, M_y and M_u are the cracking, yielding and ultimate moments; and φ_{cr}, φ_y and φ_u are corresponding curvatures.

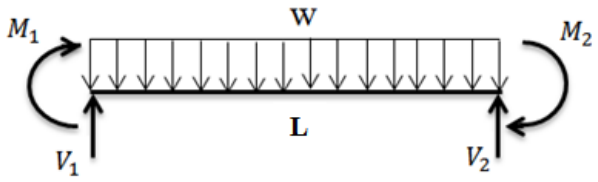

Fig. 5 The considered member to extract formulation

4. Real flexibility distribution for reinforced concrete members

Since sections along a reinforced concrete element exhibit different flexibility characteristics depending on the degree of inelasticity, in this study, the flexibility distribution assumed in the IDARC program (Fig. 3) is evaluated. For this purpose, real flexibility distributions of elements are determined and compared with those resulting from the IDARC. Real distribution is determined considering uniform distributed load that is the most probable kind of gravity loads in the building frames. In Fig. 5, the member under subjected loads and moments are taken into account to develop the formulation.

For the member shown in Fig. 5, the amount of moment in each section can be calculated by Eq. (2).

$$M(x) = V_1 x + M_1 - 0.5Wx^2 \tag{2}$$

Where, $M(x)$ is the moment in the section at a distance x from the left end. M_1 is the bending moment at the left end of the member. W is the amount of uniform distributed gravity load. V_1 is the shear force at the left end of the member and is determined according to the following equation

$$V_1 = 0.5WL - \frac{\left(M_1 + M_2\right)}{L} \tag{3}$$

Where, M_2 is the bending moment at the right end of the member. L is the length of the member.Now, to obtain the real plasticity of member, it is necessary that the flexibility of each part of member be determined. To do so, by considering moment curvature relations in section (3) and solving the following equations, different parts of member with various behaviors are specified.

(a) Locations of cracking moments in the length of the member

$$V_1 x_{cr+} + M_1 - 0.5Wx_{cr+}^2 = M_{cr+} \tag{4}$$

$$V_1 x_{cr-} + M_1 - 0.5Wx_{cr-}^2 = M_{cr-} \tag{5}$$

(b) Locations of yielding moments in the length of the member

$$V_1 x_{y+} + M_1 - 0.5Wx_{y+}^2 = M_{y+} \tag{6}$$

$$V_1 x_{y-} + M_1 - 0.5Wx_{y-}^2 = M_{y-} \tag{7}$$

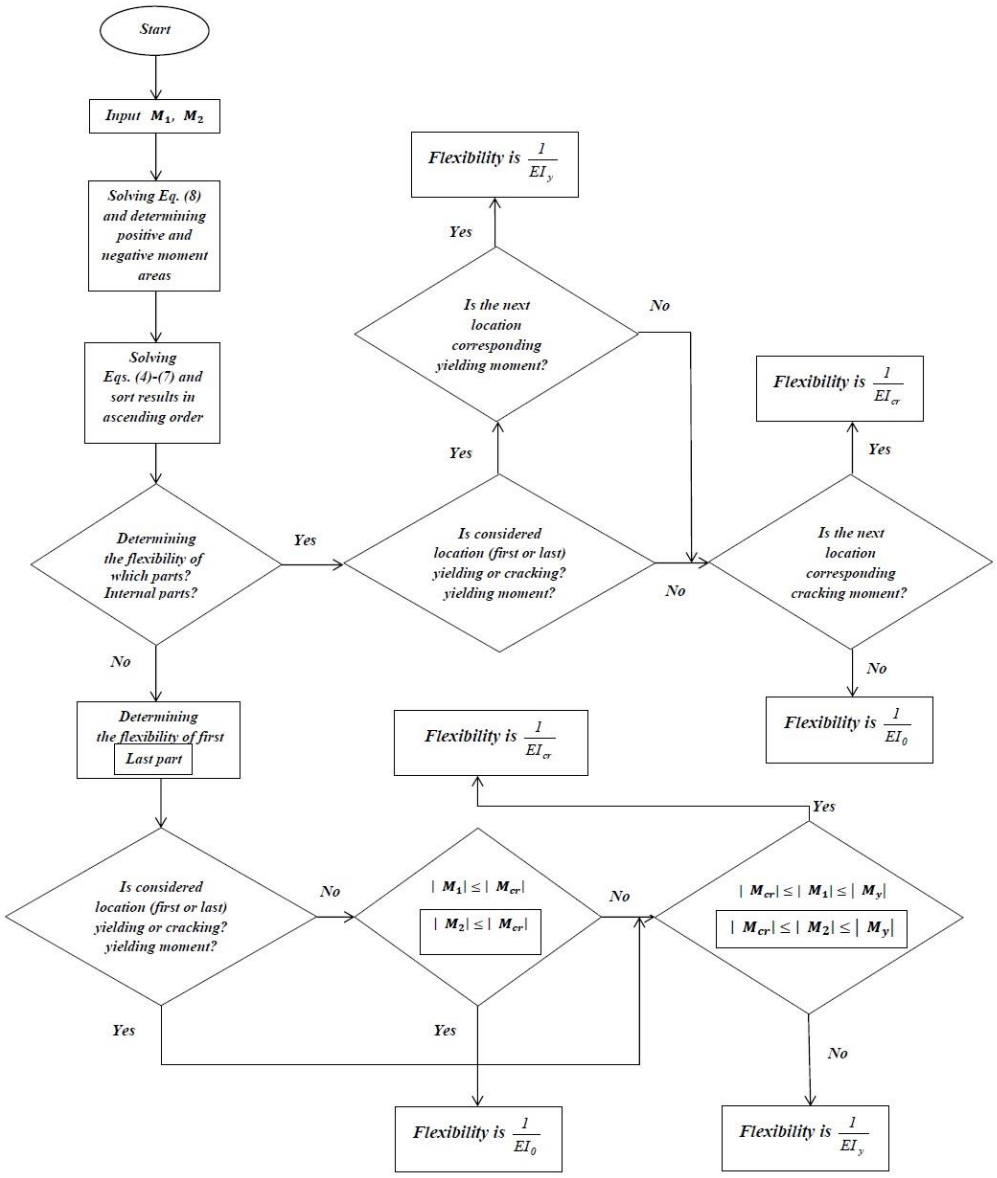

Fig. 6 The process for determining real flexural flexibility

(c) Locations of zero moments in the length of the member

$$V_1 x_0 + M_1 - 0.5 W x_0^2 = 0 \tag{8}$$

Where, x_{cr+} and x_{cr-} are the locations of positive and negative cracking moments (M_{cr+}, M_{cr-}), x_{y+} and x_{y-} are the locations of positive and negative yielding moments (M_{y+}, M_{y-}), respectively. x_0 is the location of zero moments. It should be noted that each equation from 4 to 8 can have zero, one or two roots.

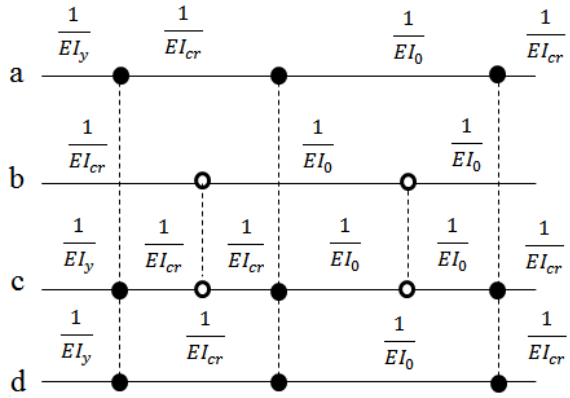

Fig. 7 Distribution of the flexural flexibility (a) step nth (b) step (n+1)th with neglecting the previous step (c) step (n+1)th with considering the previous step (d) final distribution of flexibility in which parts beside with same flexibility are assembled one

After determining the cracking and yielding points, the structural element is divided to several parts. Flexibility of each part depends on the moments in two ends of it. To determine the real flexural flexibility of each subdivided part, the following steps need to be performed:

1. Determining the number of zero moments in the moment diagram arranging from 0 to 2. This step specifies the general shape of moment diagram and is used to assign flexibility of each part.

2. Solving the equations 4 and 6 to assign the locations of positive cracking and yielding moments.

3. Solving the equations 5 and 7 to assign the locations of negative cracking and yielding moments.

4. Specifying the points determined in the two previous steps on the length of member and delimiting the length of the member between two successive points as a part.

5. Determining the flexural flexibility for internal subdivided parts based on the amount of moments in two ends. For the first part, the flexibility depends on M_1 and the moments in its right end; for the last part, the flexibility is related to M_2 and the moments in its left end. For example, if $M_{cr+} \leq M_1 \leq M_{y+}$ and the first limiting point corresponds with positive yielding moment and the number of zero points is 1, the flexural flexibility would be $\frac{1}{EI_{cr}}$. To better explain the core steps for determining the real flexural flexibility of each subdivided part, a flowchart is presented in Fig. 6. Since several different states can be occurred, to take all of them into account, a computer program called Real Flexibility Model (RFM) was prepared. In this program, all various conditions for flexural flexibility of a part of the member that can experience based on the moments of its two ends are forecast.

It should be noted that in step by step nonlinear analysis of reinforced concrete structural elements, the flexural flexibility in each step completely depends on the previous steps. Therefore, in this study two main assumptions are considered: 1. The cracked part of member does not change to a part with no crack 2. The yielded part of member does not change to a part with no crack and no yield. To consider the above mentioned matter, the current state of each member is compared with its previous state and then the flexural flexibility is obtained. Given that the

flexibility distributions of a member in two consequence steps of its analysis be like Figs. 7(a) and 7(b) (independent of previous steps); therefore, considering previous steps, the (n+1)th distributed flexibility will be similar to Fig. 7(c). The last but not the least (Fig. 7(d)) is the final flexibility distribution in which the parts with the same flexibility are taken as one part.

5. Evaluating the linear flexibility model of IDARC

Part In this section, the accuracy of the linear plasticity model used by the program IDARC is assessed. In this regard, two building frames that have been previously studied by Habibi (2007) and Habibi and Moharrami (2010) are chosen. Pushover analysis is carried out on these frames by applying monotonically increasing lateral loads along with constant gravity loads. At each load step, the base shear increment is applied to the structure with a predefined profile over the height of the structure. The incremental lateral load vector can be computed as

$$\Delta P_E = \Delta V_b \cdot \begin{Bmatrix} c_{v,1} \\ c_{v,2} \\ M \\ c_{v,ns} \end{Bmatrix} = \Delta V_b \cdot C_v \tag{9}$$

Where ΔV_b is the incremental base shear and C_v is the vector of lateral load distribution factors $\underline{C}_{v,s}$ (s=1,…, number of stories), which is determined from FEMA273

$$c_{v,s} = W_s H_s^k \Big/ \sum_{s=1}^{ns} W_s H_s^k \quad , s = 1,...,ns \tag{10}$$

Where W_s is the portion of the building seismic weight at story level s; H_s is the vertical distance from base of the building to story level s; ns is the number of stories; and k is a parameter that has been recommended by FEMA273 as follows

$$k = \begin{cases} 1 & T \prec 0.5 \\ 0.5T + 0.75 & 0.5 \le T \le 2.5 \\ 2 & T \succ 2.5 \end{cases} \tag{11}$$

Where T is the fundamental period of the building. This analysis is done by IDARC software (Valles *et al*. 1996). Since the main objective of this research is evaluating the accuracy of linear flexibility model (LFM), it is necessary that all required input parameters for each member in IDARC2D and the proposed method of this study be same. To do so, after pushover analysis by IDARC, the end moments of each member are obtained and are used to calculate the real flexibility by the proposed method. To consider various performance levels, the states of frames are taken into account regarding to overall drifts 0.5,1,2 and 4 percent in pushover analysis. The former frame is a three-story, two-bay planar asymmetric frame of Fig. 8. The concrete is assumed to have a cylinder strength of 20 Mpa, a modulus of rupture of 2.82 Mpa, a modulus of elasticity of 22360 Mpa, a strain of 0.002 at maximum strength and an ultimate strain of 0.003. The steel has a yield strength of 300 Mpa and a modulus of elasticity of 200,000 Mpa. A uniformly distributed gravity load of 20 KN/m is applied on the beams of each story. Reinforcements have the cover to the steel centroid of 50 mm. It is assumed that columns and beams have rectangular cross sections Habibi (2007).

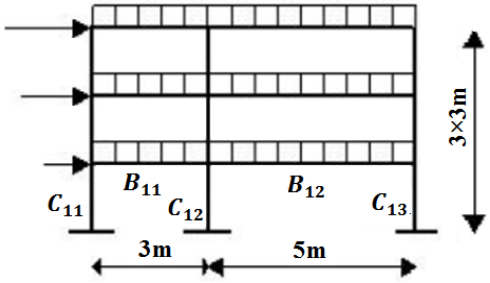

Fig. 8 The three-story frame

Table 1 The moment-curvature properties of members chosen in example 1

Member	M_{cr}(+) (KN.m)	M_{cr}(-) (KN.m)	M_y(+) (KN.m)	M_y(-) (KN.m)	EI(+) (KN. m^2)	EI(-) (KN. m^2)	EI_{cr}(+) (KN. m^2)	EI_{cr}(-) (KN. m^2)	EI_y(+) (KN. m^2)	EI_y(-) (KN. m^2)
Column										
C_{12}	28.4	28.4	80.7	80.7	17795	17795	5013	5013	135.4	135.4
C_{33}	17	17	55	55	17795	17795	4238	4238	200	200
Beam										
B_{12}	15	15	49	49	17795	17795	4100	3993	204	204
B_{21}	15	15	49	49	17795	17795	4100	3993	204	204

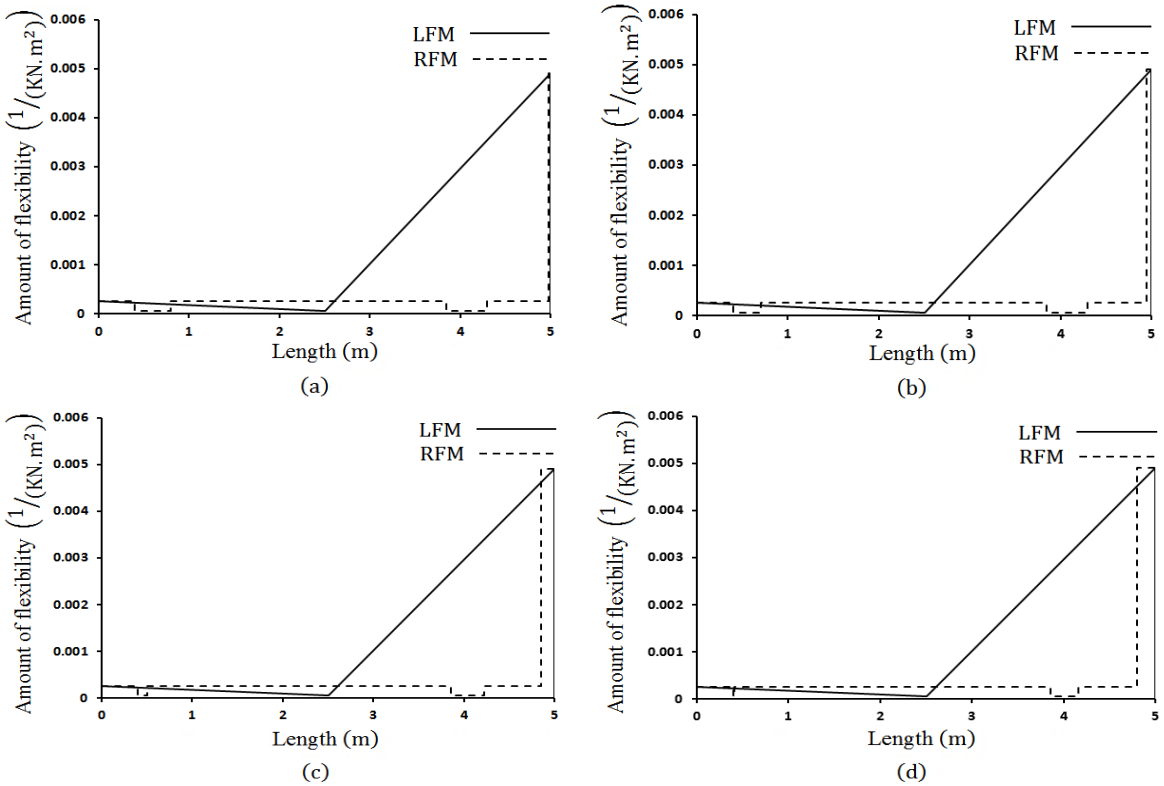

Fig. 9 LFM and RFM for B_{12} (a) overall drift is 0.5% (b) overall drift is 1% (c) overall drift is 2% (d) overall drift is 4%

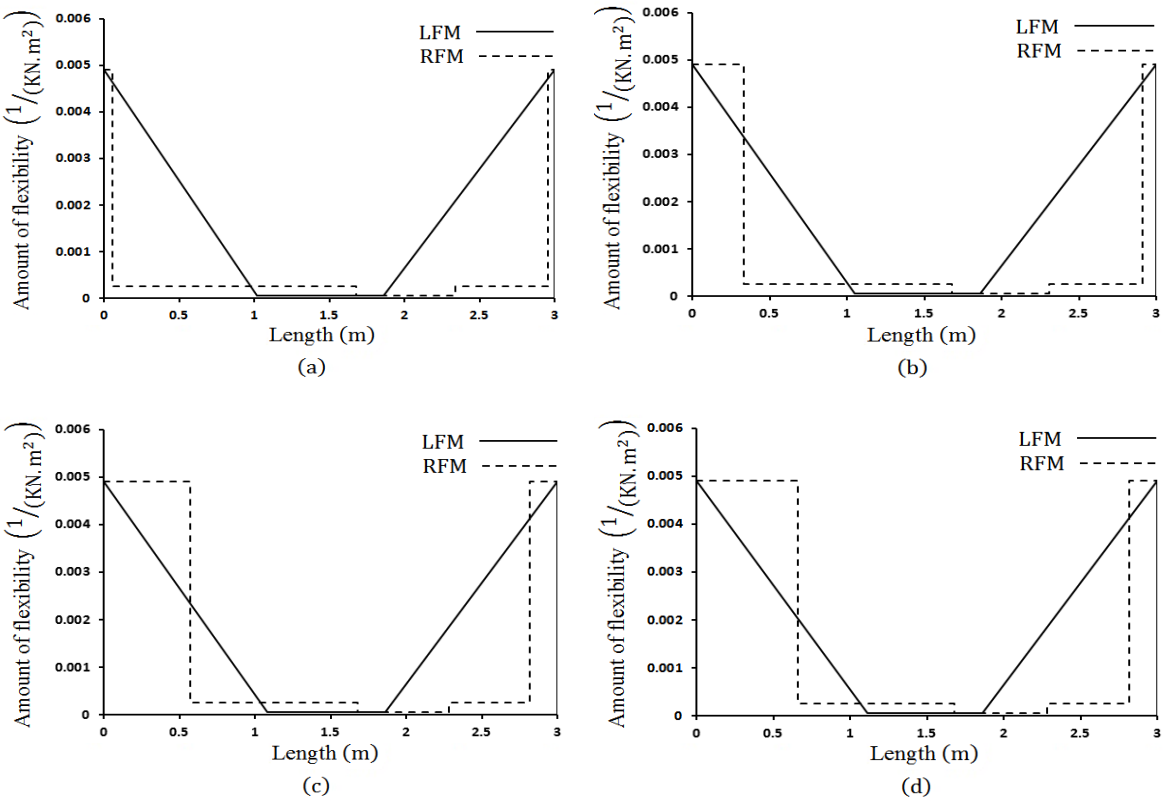

Fig. 10 LFM and RFM for B_{21} (a) overall drift is 0.5% (b) overall drift is 1% (c) overall drift is 2% (d) overall drift is 4%

As shown, numbering of elements in each story is from left to right. Therefore, the name of each member consists of two indices (like C_{ij} for columns and B_{ij} for beams) the former shows the story of the member and the latter corresponds to its place in each story. To cover varied situations in the three story frame, two beams and two columns are chosen (C_{23}, C_{33}, B_{12}, B_{21}) The moment-curvature properties of members chosen are presented in Table 1.

The linear and real flexibility distributions are shown in Figs. 9-12. In the Fig. 13, all the bending moment curves resulting from pushover analysis for each member in drift 4% are shown to express the range of end moments, cracked and yielded points and shape of moment diagrams. Since the number of curves is too many and marked points are not clear in the Fig. 13; to explain more, the bending moment curves of the first member (B_{12}) is exhibited for some moments (approximately 5 percent of moment diagrams (Fig. 13(a))). In Fig. 13, asterisk points are related to moments that are equal to positive or negative cracked moments. Diamond shapes show the location of positive or negative cracked moments and the circles are taken into account as the place of zero moments. The parameters of plasticity models are explained in Table 2. In the mentioned Table, there are two amounts for linear plasticity model presenting the yield penetration coefficients (Fig. 3). For the real flexibility model, there are some coefficients expressing the transformation points. It should be noted that these mentioned points are calculated from the left side and all these lengths are divided to the length of members.

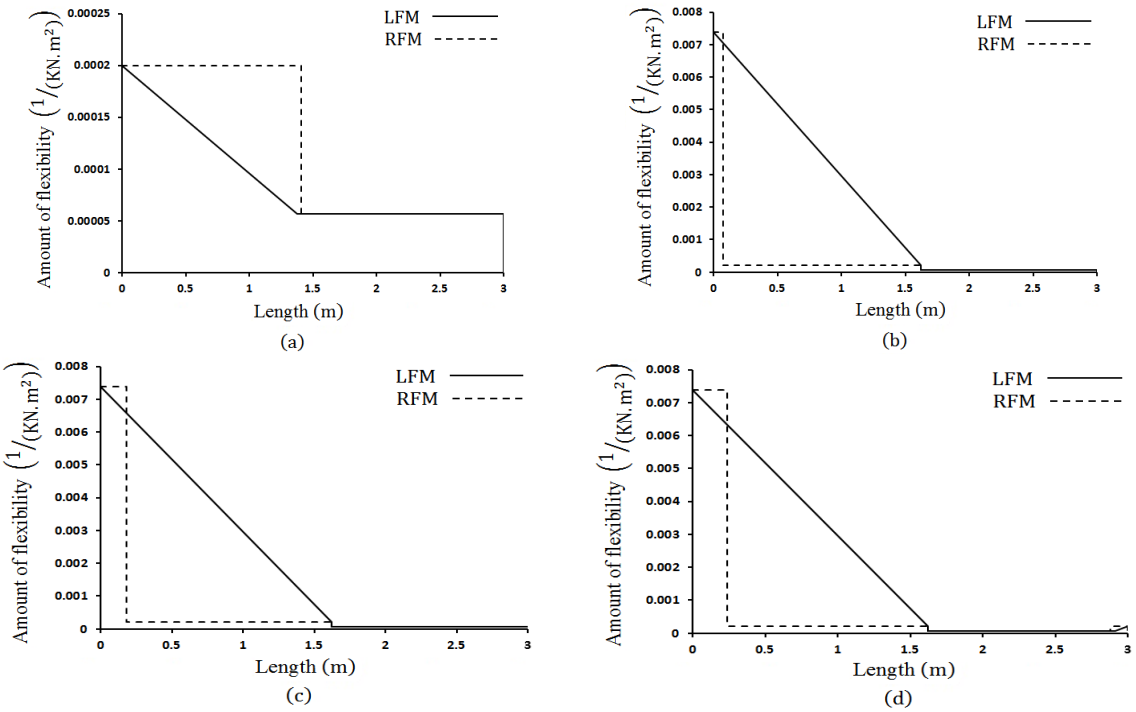

Fig. 11 LFM and RFM for C_{12} (a) overall drift is 0.5% (b) overall drift is 1% (c) overall drift is 2% (d) overall drift is 4%

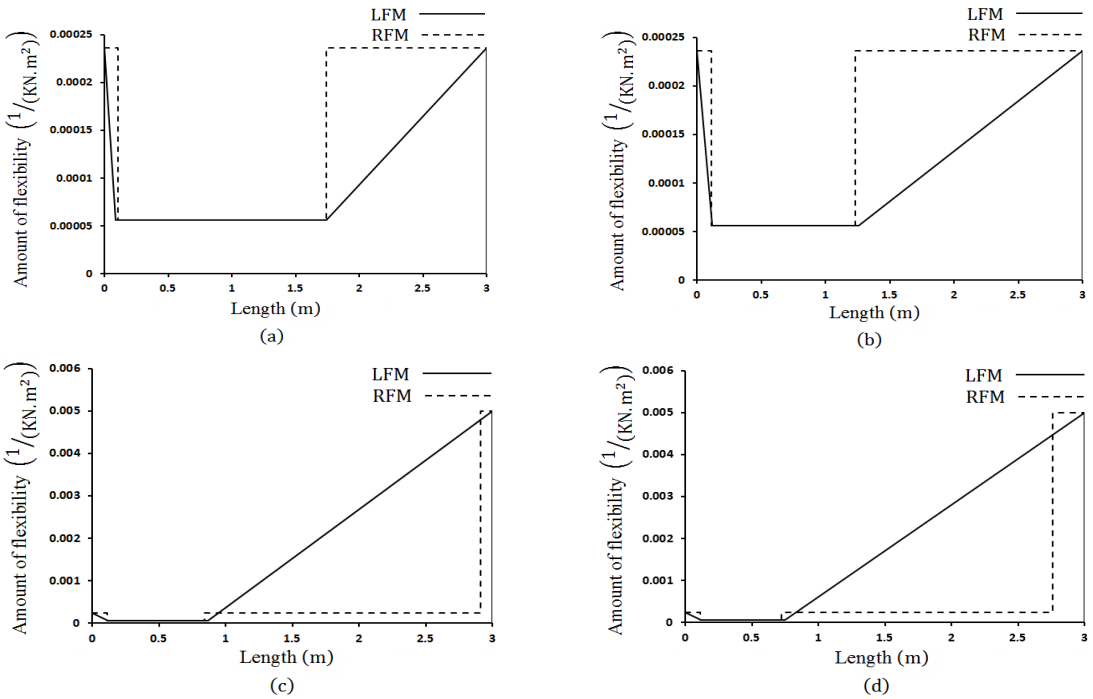

Fig. 12 LFM and RFM for the element C_{33} (a) overall drift is 0.5% (b) overall drift is 1% (c) overall drift is 2% (d) overall drift is 4%

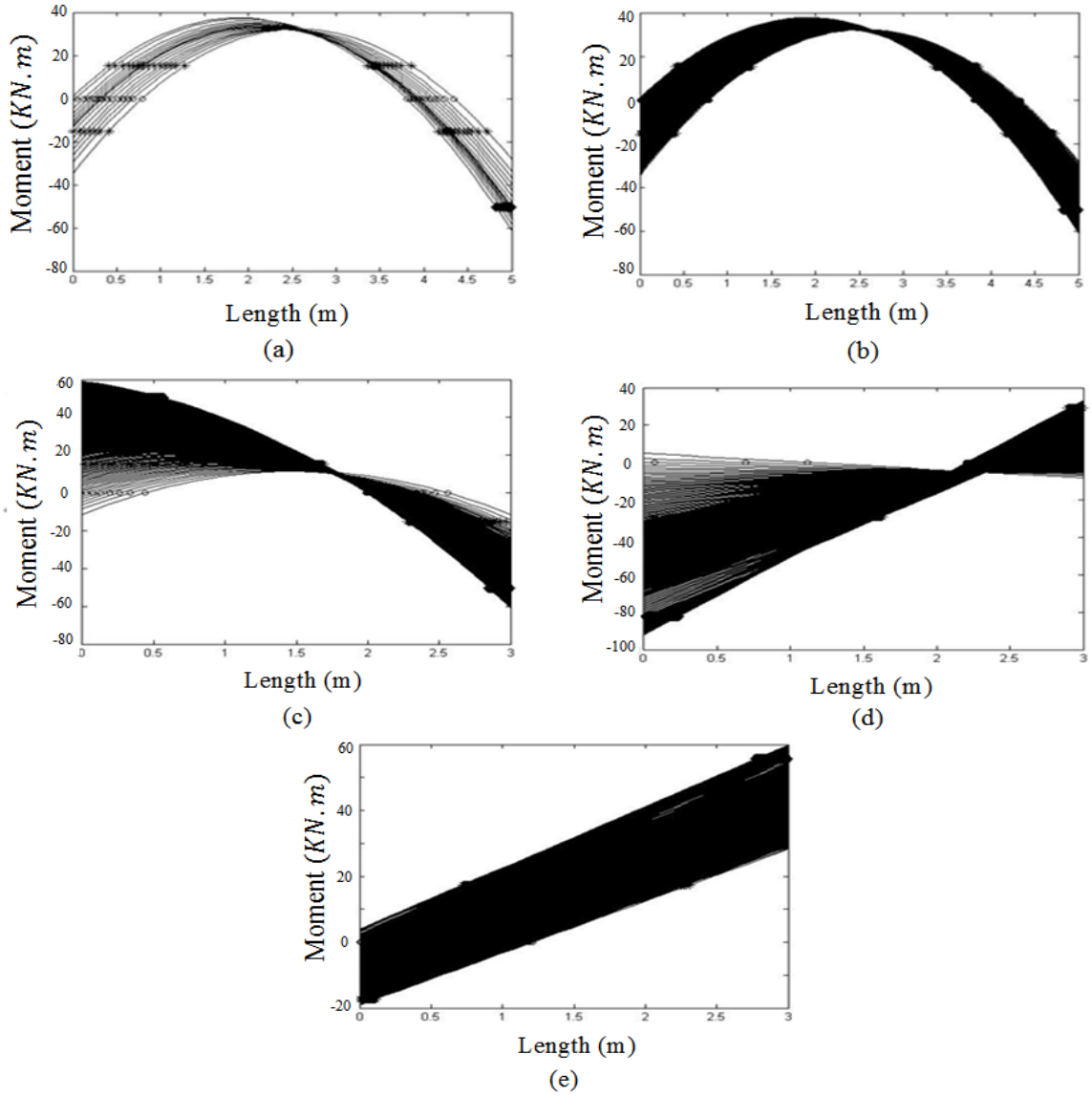

Fig. 13 The bending moment diagrams for the selected members in example 1 (a) the 5 percent of all moment diagrams for B_{12}. (b-e) all of moment diagrams for B_{12}, B_{21}, C_{12} and C_{33} respectively

As shown in Figs. 9-12, in all the members at various performance levels, the linear plasticity model could not reflect the real flexibility of them. For B_{12}, it is clear that the linear flexibility model (LFM) is more flexible than the real one. This can lead to more rotation in the right side of member which directly affects the performance levels. It seems that for the right side of this member, the power spread plasticity model proposed by Roh *et al*. (2012), may model the flexibility more proper than LFM. As evident for B_{21}, LFM in the end right side of the length of member is stiffer than RFM. In the left side, the flexibility of LFM is lower than RFM in the part near the end but, in the middle part, the flexibility is more. For the right side of this element, it

seems that the power plasticity model with high power will be more accurate than LFM as long as the length of the yielded part is restricted; but as shown, when the length of the yielded part increases like the left side of B_{21} in drift 4%, the power plasticity model with low power can model the flexibility well. The results presented for beam elements in the first example are completely different in linear and real flexibility models. Since LFM does not take the gravity loads into account, this model can make egregious errors. What is manifest for beam elements is that although power spread plasticity can increase the accuracy of flexibility, the main problem is neglecting gravity loads; therefore, for beams, the places of cracked and yielded points are different from real locations. Also, the power in power spread plasticity simply depends on the end moments and cannot consider the effects of gravity loads in the middle parts of the beam elements. The flexibility models for C_{12} are different as well. Although for the overall drift 0.5%, LFM is stiffer than RFM, for the other performance levels it is more flexible except for the yielded part narrowed in the end of left side. For the last member C_{33}, the LFM is stiffer than RFM in the two prime performance levels. Unlike first and second performance levels, the linear flexibility distribution for the both of last performance levels is more flexible than real flexibility distribution except in the small end yielded part of right side that is stiffer. As shown, the LFM even the column members that are just subjected to lateral loads, cannot reflect the real flexibility of them. It seems because of lack of gravity loads on the column elements, the power flexibility model can model the flexibility more accurately.

In this example, some performance levels were assessed and the accuracy of them was challenged. It should be noted that the effect of errors occurred is noticeable in some analyses like dynamic, cyclic and pushover methods because the stiffness or softness matrix of a structure depends on the flexibility models used in them. The errors of the flexibility models accumulated in the steps of the analysis are not negligible. This matter will be described more in the next example.

The latter example is a ten-story, two-bay planar frame of Fig. 14. For this example, the concrete is assumed to have a cylinder strength of 30 Mpa, a modulus of rupture of 3.45 Mpa, a modulus of elasticity of 27,400 Mpa, a strain of 0.002 at maximum strength and an ultimate strain of 0.004. The other material properties are same with the first example. A uniformly distributed gravity load of 20 KN/m is applied on the beams of each story. Reinforcements have the cover to the steel centroid of 50 mm. It is assumed that columns and beams have rectangular cross sections (Habibi and Moharrami 2010).

Table 2 Yield penetrations coefficients for LFM and the transformation points for RFM in example 1

Overall drift %	*Linear flexibility model*				*Real flexibility model*			
	C_{12}	C_{33}	B_{12}	B_{21}	C_{12}	C_{33}	B_{12}	B_{21}
0.5	0.46,0	0.03, 0.42	0.5, 0.5	0.34, 0.38	0.47	0.036, 0.58	0.08,0.16, 0.77, 0.86,0.998	0.018,0.56, 0.78, 0.986
1	0.54,0	0.04, 0.58	0.5, 0.5	0.35, 0.38	0.025, 0.54	0.037, 0.41	0.08,0.14, 0.77, 0.86,0.99	0.11,0.56, 0.77, 0.97
2	0.54,0	0.04, 0.71	0.5, 0.5	0.36, 0.38	0.06, 0.54	0.037,0.28, 0.97	0.08,0.10, 0.772, 0.844,0.97	0.19,0.56, 0.76, 0.94
4	0.54,0.03	0.04, 0.75	0.5, 0.5	0.37, 0.38	0.08,0.54, 0.96	0.037,0.24, 0.92	0.08,0.082, 0.772, 0.833,0.96	0.22,0.56, 0.76, 0.94

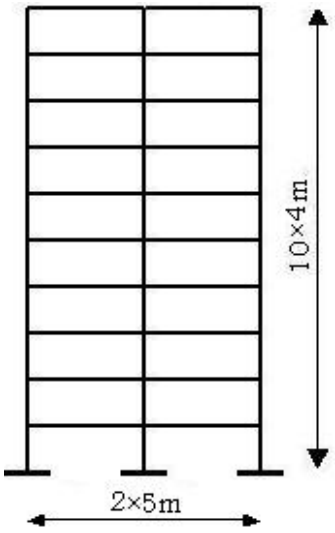

Fig. 14 The ten-story frame

Table 3 The moment-curvature properties of members chosen in example 2

Member	M_{cr}(+) (KN.m)	M_{cr}(-) (KN.m)	M_y(+) (KN.m)	M_y(-) (KN.m)	EI(+) (KN. m^2)	EI(-) (KN. m^2)	EI_{cr}(+) (KN. m^2)	EI_{cr}(-) (KN. m^2)	EI_y(+) (KN. m^2)	EI_y(-) (KN. m^2)
Column										
C_{21}	91.4	91.4	719	719	339230	339230	200771	200771	2825	2825
C_{72}	49.1	49.1	240	240	45705	45705	24820	24820	363	363
Beam										
B_{32}	87	87	474	474	217340	217340	97943	99473	1618	1618
B_{91}	13.7	13.7	88.3	88.3	17207	17207	7642	7809	284	284

Table 4 Yield penetrations coefficients for LFM and the transformation points for RFM in example 2

Overall drift %	***Linear flexibility model***				***Real flexibility model***			
	C_{21}	C_{72}	B_{32}	B_{91}	C_{21}	C_{72}	B_{32}	B_{91}
0.5	0.129, 0	0.36, 0.32	0.26, 0.38	0.5, 0.5	0.126	0.35,0.67	0.38, 0.726	0.998
1	0.37, 0.13	0.40, 0.36	0.31, 0.42	0.5, 0.5	0.36, 0.87	0.40,0.63	0.4, 0.66	0.98
2	0.44, 0.20	0.43, 0.362	0.34, 0.42	0.5, 0.5	0.43, 0.79	0.005, 0.43, 0.63	0.42, 0.65	0.96
4	0.48, 0.25	0.43, 0.363	0.35, 0.43	0.5, 0.5	0.46, 0.74	0.015, 0.43, 0.635	0.426, 0.64	0.95

In this frame, four members including two beams and two columns just like the first frame (B_{32}, B_{91}, C_{21}, C_{72}) are chosen. The moment-curvature properties of the members are expressed in Table 3.

The plasticity models are presented in Figs. 15-18 and the related plasticity parameters are described in Table 4.

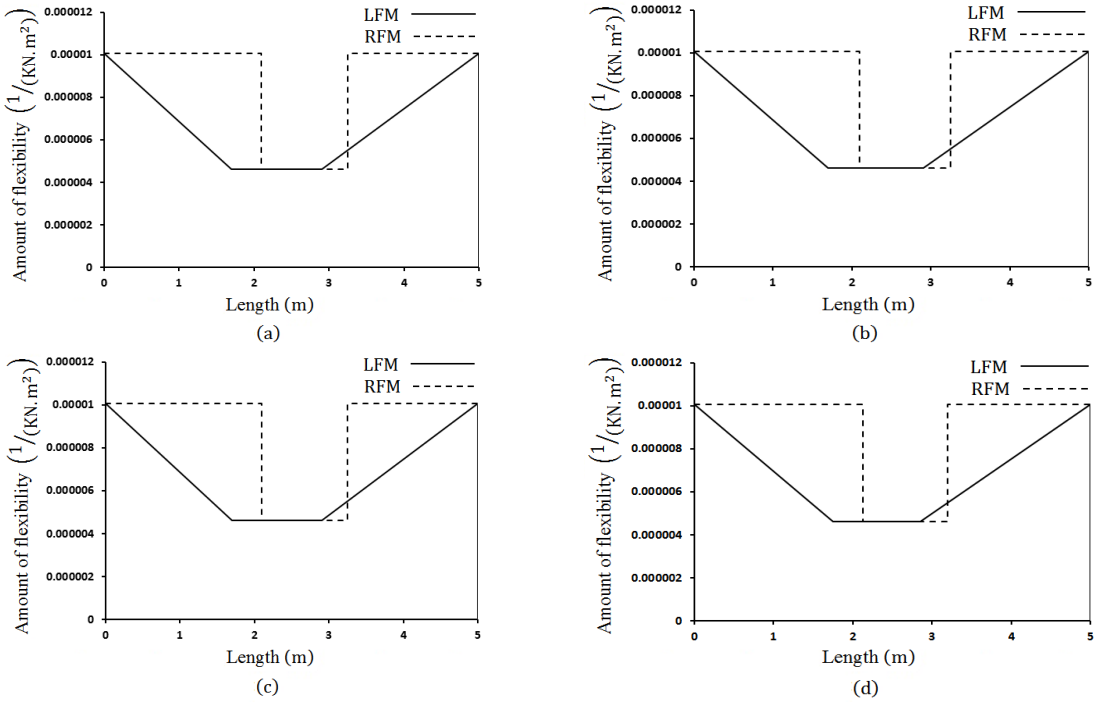

Fig. 15 LFM and RFM for B_{32} (a) overall drift is 0.5% (b) overall drift is 1% (c) overall drift is 2% (d) overall drift is 4%

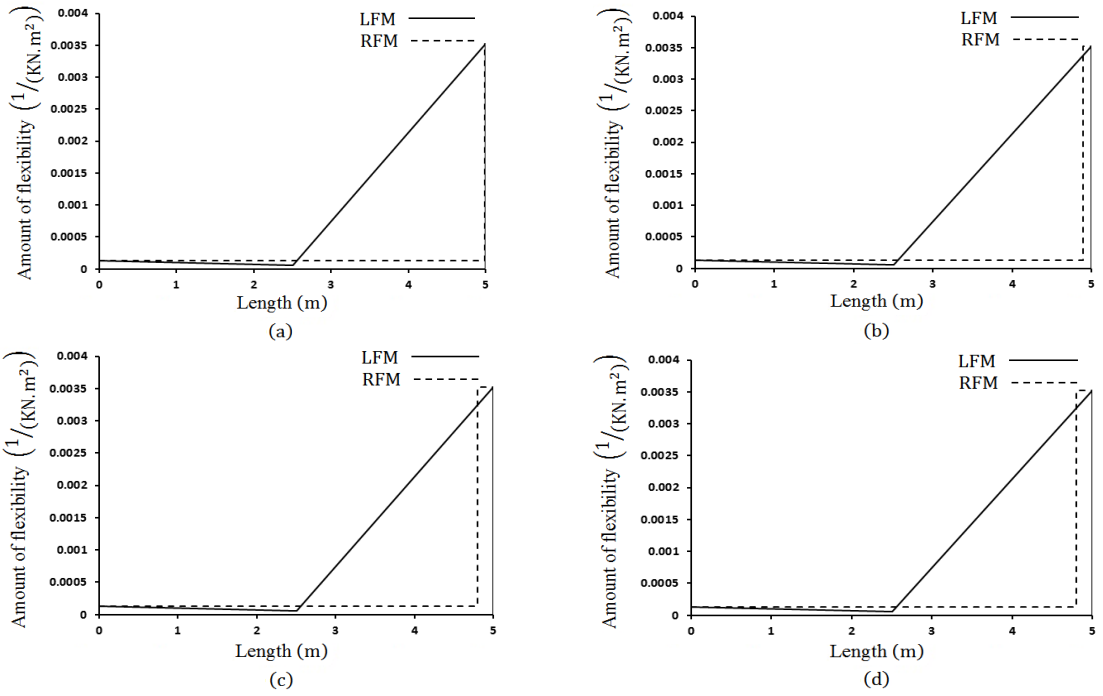

Fig. 16 LFM and RFM for B_{91} (a) overall drift is 0.5% (b) overall drift is 1% (c) overall drift is 2% (d) overall drift is 4%

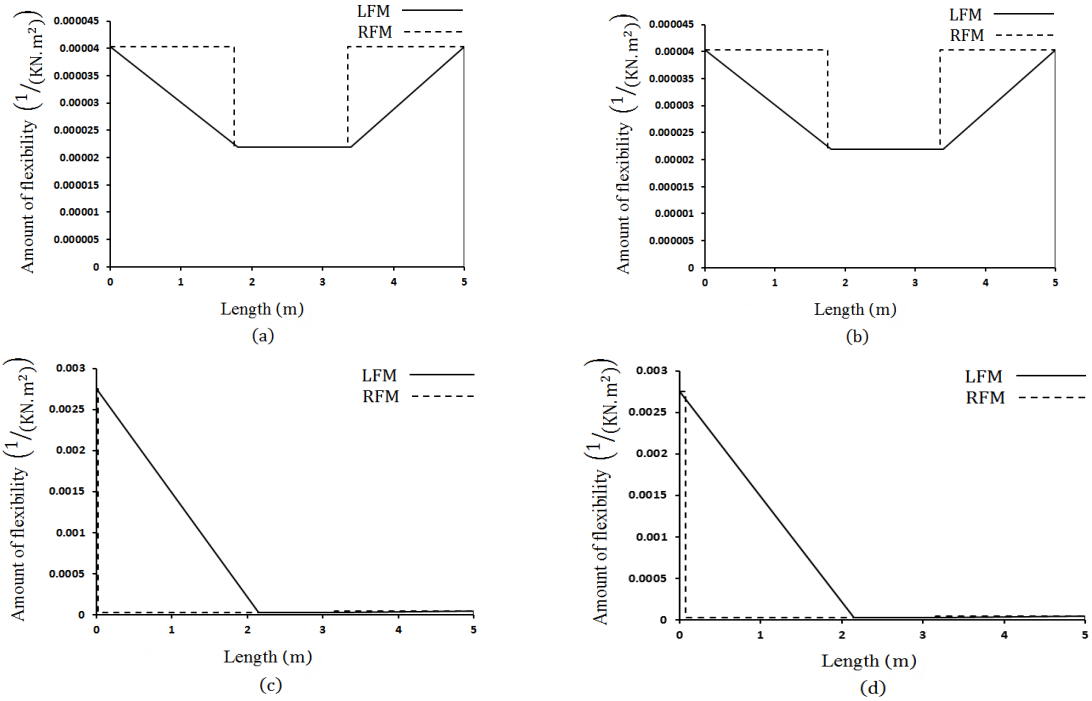

Fig. 17 LFM and RFM for C_{72} (a) overall drift is 0.5% (b) overall drift is 1% (c) overall drift is 2% (d) overall drift is 4%

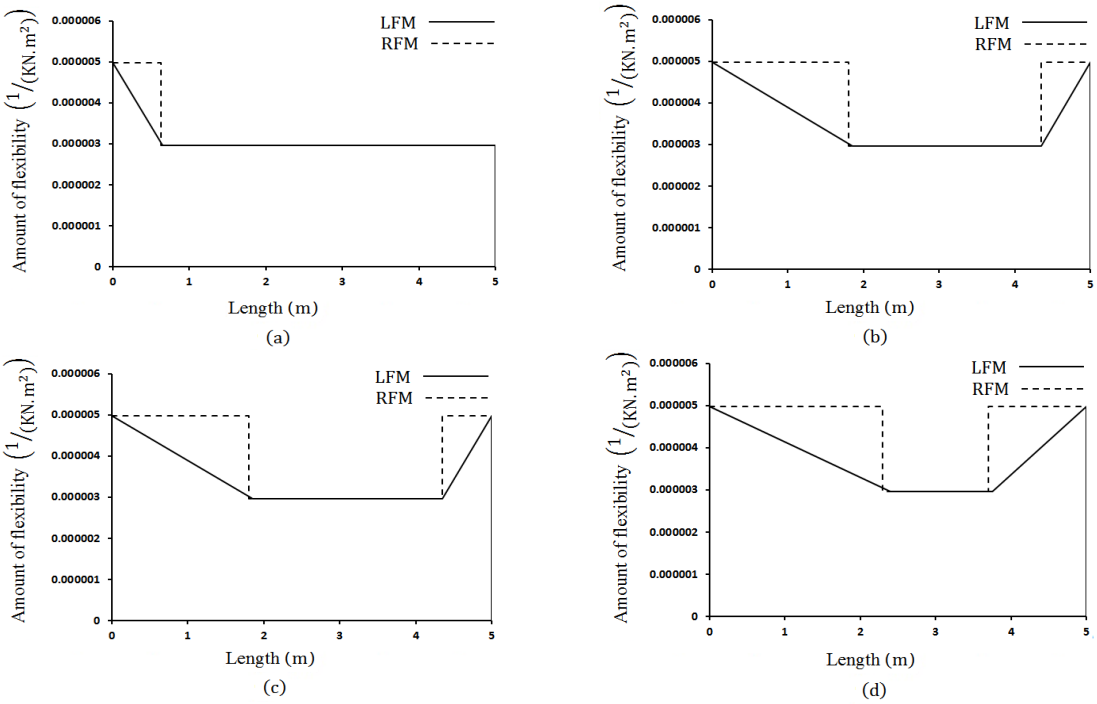

Fig. 18 LFM and RFM for C_{21} (a) overall drift is 0.5% (b) overall drift is 1% (c) overall drift is 2% (d) overall drift is 4%

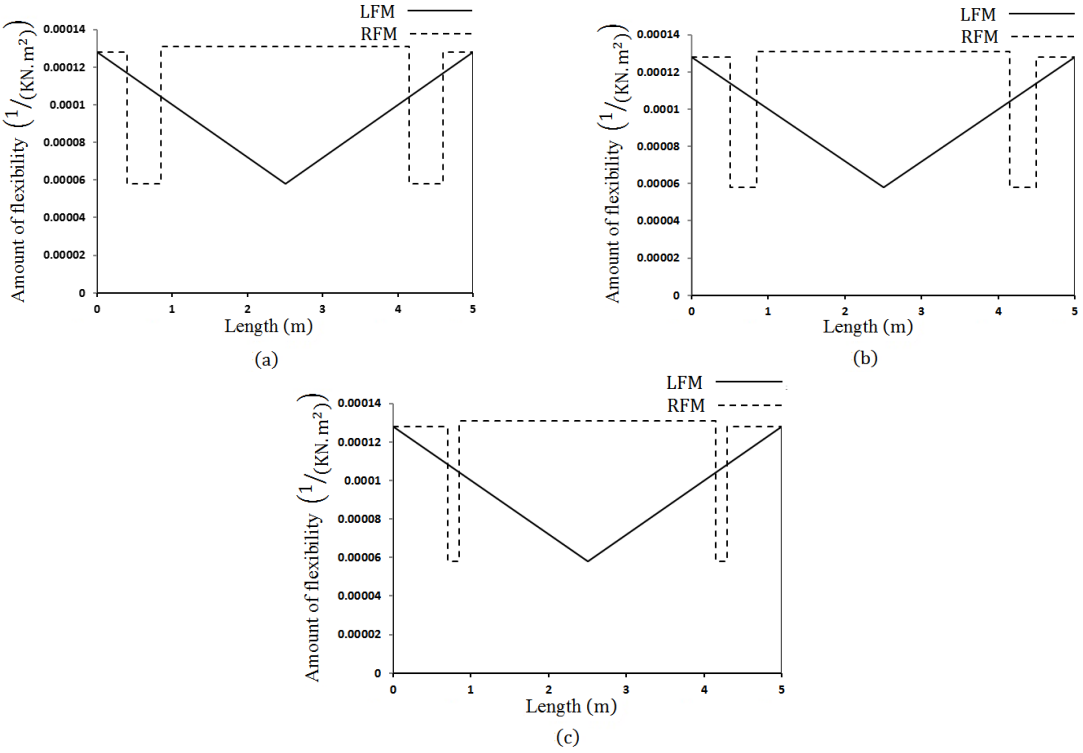

Fig. 19 LFM and RFM for B_{91} (a) overall drift is 0.05% (b) overall drift is 0.1% (c) overall drift is 0.2%

As can be seen, in the second example, also, the highest difference between the real and linear flexibility models is related to the beam elements. Neglecting the gravity loads in LFM brings about errors in the location of the cracked and yielded moments (this problem exists in other models like the power plasticity model disregarding the effect of gravity loads). For B_{32}, the linear flexibility model is stiffer than real one. The gap between the models for B_{91} is very large and the LFM is more flexible than RFM. Occurring yield in the left side of C_{72} leads to a large contrast between the two models. For the last member C_{21}, in all the overall drifts, LFM is more flexible than RFM. As noted, the accumulated errors of the flexibility models severely affect the outcomes of analysis. For more explanation, several steps of pushover analysis of B_{91} are presented. These steps are regarding the 0.05, 0.1 and 0.2 percent overall drifts. These drifts are chosen to show the influence of neglecting the gravity loads (Fig. 19).

As shown, in the 0.05, 0.1 and 0.2 percent overall drifts, middle part of the beam is cracked. The gap between LPM and RPM is very large. None of the plasticity models when ignoring the gravity loads cannot correctly simulate the flexibility of beams in most steps of analyses. This occurs in the steps in which the effect of gravity loads overcomes the lateral moments. Although in some analyses like pushover analysis, the effect of lateral loads dominate the gravity loads by increasing the overall drift, the stiffness matrix depends on the plasticity models in all steps of analysis; therefore, the accumulated errors in initial steps of analysis can lead to big errors in the next steps.

It should be noted that despite improving the accuracy of some models like “multi segment model” when increasing the number of segment, these models have some problems. In the

mentioned model, the more accurate flexibility is obtained when shorter segments are chosen. These shorter segments require more computational effort that is time consuming. Moreover, in some steps of analyses, it is possible that the behavior of elements still is elastic or experience crack in the small parts of elements and therefore it is not necessary that they be subdivided into shorter segments.

6. Conclusions

In this study, the spread plasticity model of IDARC for reinforced concrete elements was evaluated. For this purpose, first, a real spread plasticity model was developed that takes the influence of gravity loads into account. In the proposed model, the flexibility of each member is determined based on the locations of positive and negative yielded and cracked flexural moments in current step of analysis and also by considering history of flexibility in previous steps. Then, the real plasticity model was compared with the linear plasticity model used in IDARC that is one of prevalent models for reinforced concrete elements. To do so, pushover analysis was carried out on a 3-story frame and a 10-story frame. To cover wide range of behavior of the frames, the plasticity models are compared in the 0.5%, 1%, 2% and 4% of overall drifts. The outcomes exhibit that the linear plasticity model has glaring errors in modeling reinforced concrete elements and can model the member stiffer or softer than real model. Some of these errors may be eliminated by using other plasticity models like the power or the uniform spread plasticity. Meanwhile other ones like the locations of cracked and yielded bending moments in beam elements subjected to gravity loads, cannot be omitted by existing models in which the gravity load effects are ignored.

References

Al-Haddad, M.S. and Wight, J.K. (1986), "Feasibility and consequences of moving beam plastic hinging zones for earthquake resistant design of R/C buildings", Report No. UMCE 86-1, The University of Michigan, Ann Arbor, Michigan.

Alva, G.M.S. and de Cresce El, A.L.H. (2010), "Application of lumped dissipation model in nonlinear analysis of reinforced concrete structures", *Eng. Struct*., **32**(4), 974-81.

Aoyama, H. and Sugano, T. (1968), "A generalized inelastic analysis of reinforced concrete structures based on the tests of members", Recent researches of structural mechanics, Contribution in Honour of the 60th Birthday of Professor Y. Tsuboi, Uno-Shoten, Tokyo, 15-30.

Birely, A.C., Lowes, L.N. and Lehman, D.E. (2012), "A model for the practical nonlinear analysis of reinforced-concrete frames including joint flexibility", *Eng. Struct*., **34**(1), 455-65.

Clough, R.W. and Johnston, S.B. (1966), "Effect of stiffness degradation on earthquake ductility requirements", *Transactions of Japan Earthquake Engineering Symposium*, Tokyo.

FEMA273 (1997), "NEHRP Guideline for the seismic rehabilitation of buildings", Federal Emergency Management Agency, Washington, DC.

Giberson, M.F. (1967), "The response of nonlinear multi-story structures subjected to earthquake excitation", Earthquake Engineering Research Laboratory, California Institute of Technology, Pasadena, CA, EERL Report.

Giberson, M.F. (1969), "Two nonlinear beams with definitions of ductility", *J. Struct. Div*., **95**(ST2), 137-57.

Habibi, A.R, (2007), "Optimal seismic performance-based design of 2D RC frameworks", Ph.D. Thesis, Tarbiat Modares University, Tehran, Iran.

Habibi, A.R. and Moharrami, H. (2010), "Nonlinear sensitivity analysis of reinforced concrete frames",

Finite Elem. Anal. Des., **46**, 571-584.
Hajjar, J.F., Molodan, A. and Schiller, P.H. (1998), "A distributed plasticity model for cyclic analysis of concrete-filled steel tube beam-columns and composite frames", *Eng. Struct*., **20**(4-6), 398-412.
Hajjar, J.F., Schiller, P.H. and Molodan, A. (1998), "A distributed plasticity model for concrete filled steel tube beam-columns with interlayer slip", *Eng. Struct*., **20**(8), 663-76.
He, R. and Zhong, H. (2012), "Large deflection elasto-plastic analysis of frames using the weak-form quadrature element method", *Finite Elem. Anal. Des*., **50**, 125-133.
Kim, S.P. and Kurama, Y.C. (2008), "An alternative pushover analysis procedure to estimate seismic displacement demands", *Eng. Struct*., **30**, 3793-3807.
Kucukler, M., Gardner, L. and Macorini, L. (2014), "A stiffness reduction method for the in-plane design of structural steel elements", *Eng. Struct*., **73**, 72-84.
Kunnath, S.K. and Reinhorn, A.M. (1989), "Inelastic three-dimensional response analysis of reinforced concrete structures subjected to seismic loads", Technical Report No. NCEER-88-0041, University at Buffalo, The State University of New York.
Nguyen, P.C. and Kim, S.E. (2014), "Distributed plasticity approach for time-history analysis of steel frames including nonlinear connections", *J. Constr. Steel Res*., **100**, 36-49.
Otani S. (1980), "Nonlinear dynamic analysis of reinforced concrete building structures", *Can. J. Civil Eng*., **7**(2), 333-44.
Park, Y.J., Reinhorn, A.M. and Kunnath, S.K. (1987), "IDARC: Inelastic damage analysis of reinforced concrete frame-shear wall structures", Technical Report No. NCEER- 87-0008, University at Buffalo, The State University of New York.
Powell, G.H. (l975), "Supplement to computer program DRAIN-2D", Supplement to report, DRAIN-2D user's guide, University of California, Berkeley, CA.
Reinhorn, A.M., Roh, H., Sivaselvan, M., Kunnath, S.K., Valles, R.E., Madan, A., Li, C., Lobo, R. and Park, Y.J. (2009), "IDARC 2D Version 7.0: A Program for the Inelastic Damage Analysis of Structures", MCEER Technical Report, MCEER-09-0006, University at Buffalo-the State University of New York.
Roh, H., Reinhorn, A.M. and Lee, J.S. (2012), "Powerspread plasticity model for inelastic analysis of reinforced concrete structures", *Eng. Struct*., **39**, 148-161.
Takizawa, H. (1973), "Strong motion response analysis of reinforced concrete buildings", *J. Jpn. Nat. Council Concrete*, **II**(2), 10-21.
Valles, R.E., Reinhorn, A.M., Kunnath, S.K., Li, C. and Madan, A. (1996), "IDARC2D Version 4.0 – a computer program for the inelastic drainage analysis of buildings", Technical Report No. NCEER-96-0010, University at Buffalo, The State University of New York.
Wen, R.K. and Janssen, J.G. (1965), "Dynamic analysis of elasto-inelastic frames", *Proceedings of 3rd World Conference on Earthquake Engineering*, 713-29.

CC